# Supporting Information for

# Two-dimensional $Be_2Au$ Monolayer with Planar Hexacoordinate s-Block Metal Atoms: A Superconducting Global Minimum Dirac Material with Two Perfect Dirac Node-Loops

Meng-hui Wang,[a] Zhong-hua Cui,*[a,e] Sheng Wang,[c] Quan Li,[c] Jijun Zhao,[d] and Zhongfang Chen*[b]

[a]*Institute of Atomic and Molecular Physic, Jilin University, Changchun 130012, China*

*E-mail: zcui@jlu.edu.cn*

[b]*Department of Chemistry, University of Puerto Rico, San Juan, PR 00931, United States*

*E-mail: zhongfangchen@gmail.com*

[c]*State Key Laboratory of Superhard Materials, College of Physics, Jilin University, Changchun 130023, People's Republic of China*

[d]*Key Laboratory of Materials Modification by Laser, Ion and Electron Beams (Dalian University of Technology), Ministry of Education, Dalian 116024, China*

[e]*Key Laboratory of Physics and Technology for Advanced Batteries (Ministry of Education), Jilin University, Changchun 130012, China*

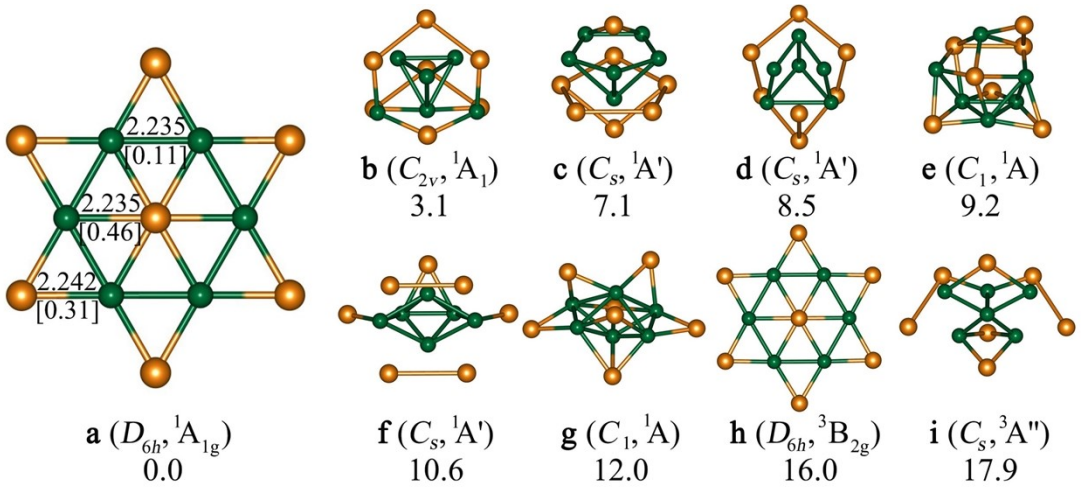


**Figure S1.** The structures and relative energies in kcal/mol of the low-lying energy isomers of $Be_6Au_7^-$ computed at the CCSD(T)/def2-TZVP//PBE0/def2-TZVP. The bond distances in Å and WBI values (in square brackets) of phAu are given. Gold and green balls represent Au and Be atoms, respectively.

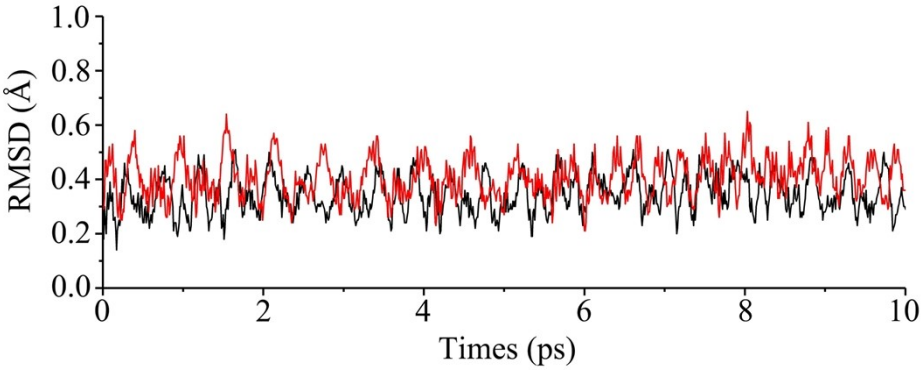


**Figure S2.** The RMSD vs simulation time of the isolated phAu $Be_6Au_7^-$ at 300K (black line) and 600K (red line) computed at the PBE0/def2-SVP level.

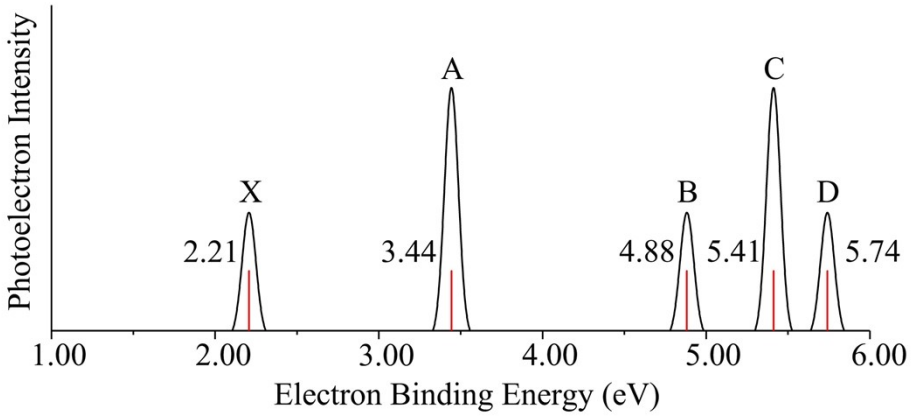


**Figure S3.** Simulated photoelectron spectroscopy (PES) of the phAu $Be_6Au_7^-$ cluster.

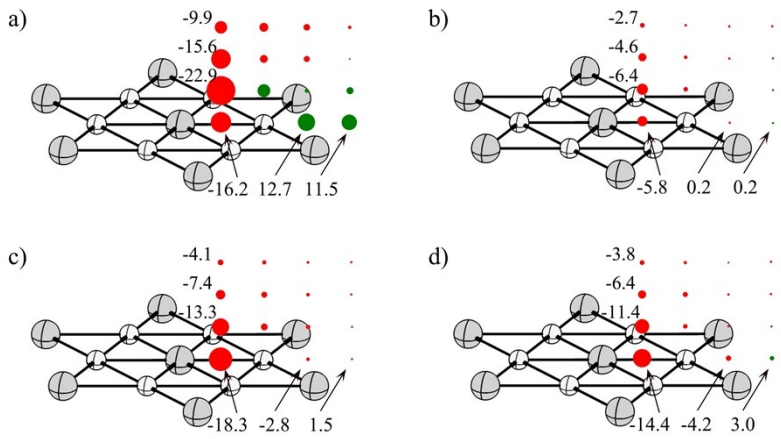


**Figure S4.** a) $NICS_{zz}$, b) $NICS_{zz}(\pi)$, c) $NICS_{zz}(\sigma\text{-delocalization})$, d) $NICS_{zz}(\sigma\text{-localization})$ of the $D_{6h}$ $Be_6Au_7^-$ at the PBE0/def2-TZVP level. Diatropic (aromaticity) and paratropic (anti-aromaticity) tensors are shown in red and green, respectively. NICS values are in ppm.

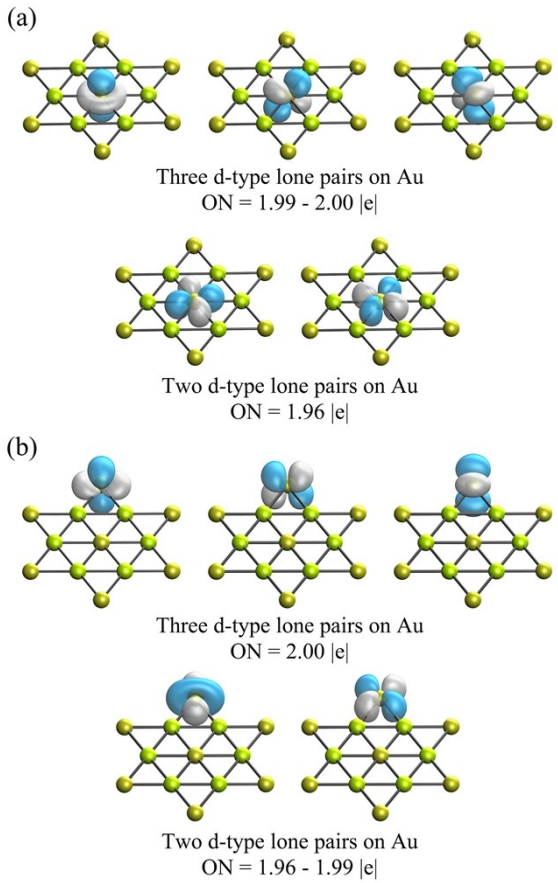


**Figure S5**. AdNDP of d-type lone pairs at a) phAu and b) bridging Au atoms.

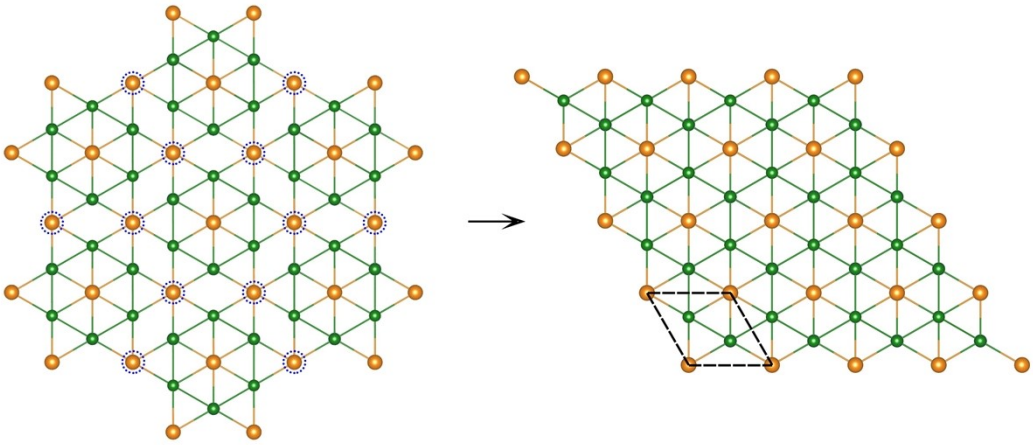

**Figure S6**. A schematic view of part of the extended 2D $Be_2Au$ monolayer as constructed from the starlike $Be_6Au_7$ unit. The circles represent the bridging Au atoms in $Be_6Au_7$ unit that are shared by three units.

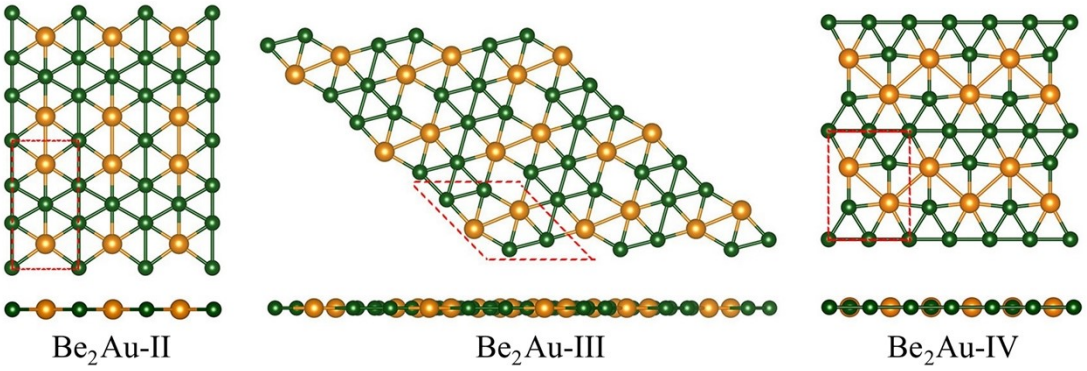


**Figure S7.** Three low-lying isomers of 2D $Be_2Au$ found by particle swarm search. Gold and green balls represent Au and Be atoms, respectively.

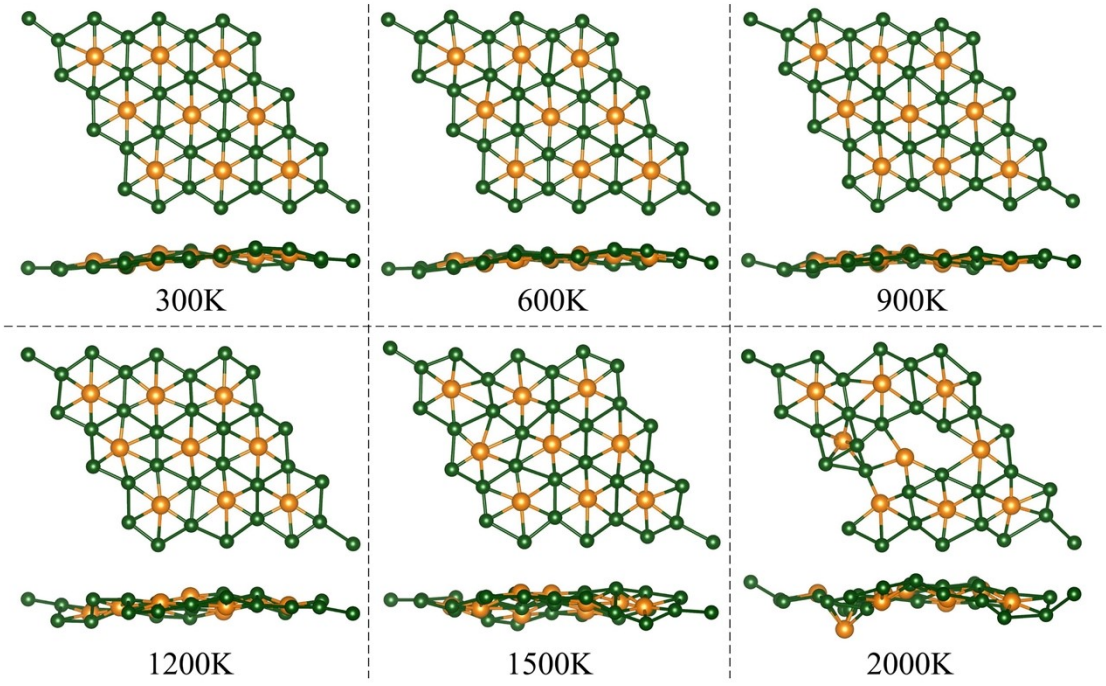


**Figure S8.** Snapshots of the equilibrium of the $Be_2Au$ monolayer from 300 to 2000K (top and side views) at the end of 10 ps based on AIMD simulation, and bonds to atoms outside this 4 × 4 section exit but are not show.

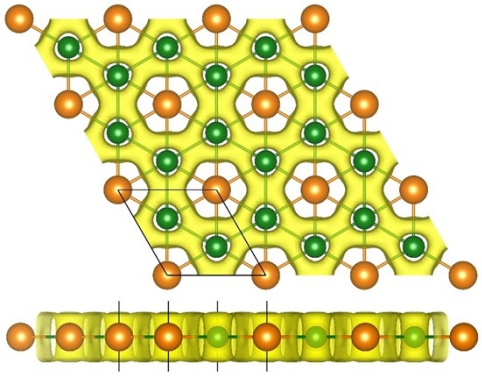

**Figure S9**. The 3D representation of ELF of $Be_2Au$ monolayer.

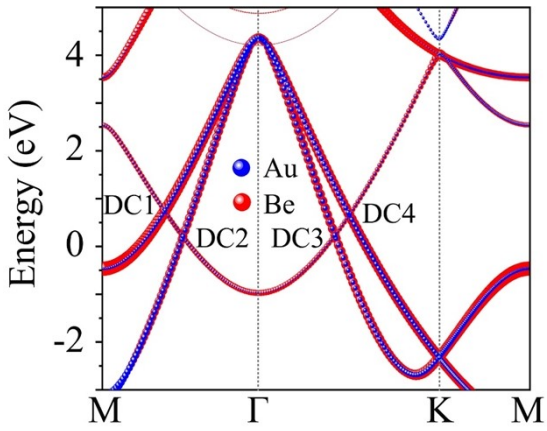


**Figure S10.** Band structure of $Be_2Au$ monolayer calculated by HSE06 functional.

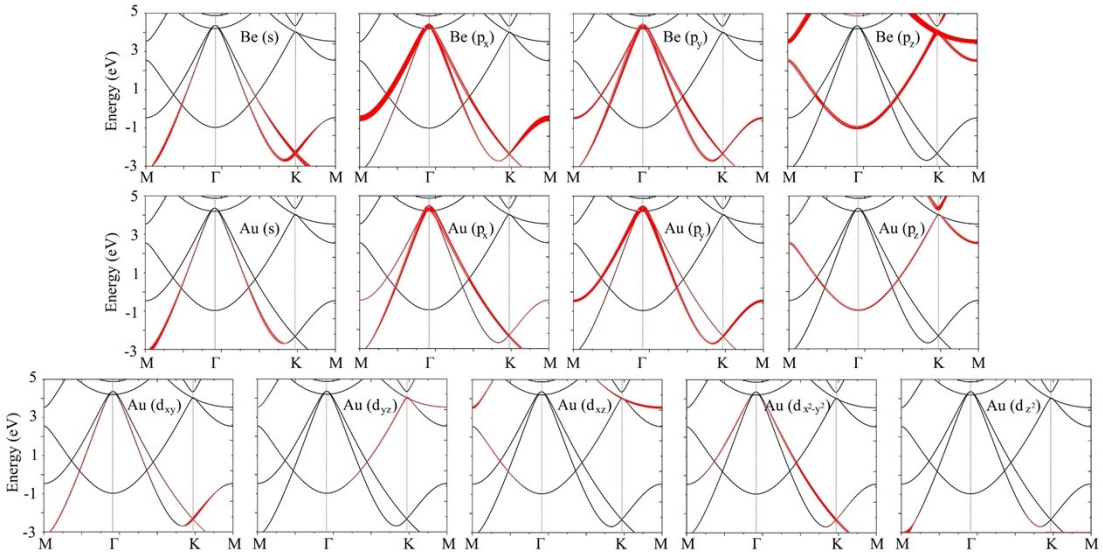


**Figure S11.** Projected band structures of $Be_2Au$ monolayer, indicating the α/β bands are contributed by in-plane orbitals: Be $p_x/p_y$, Au $p_x/p_y/d_{xy}/d_{x^2-y^2}$, and the γ band is contributed by out-of-plane orbitals: Be $p_z$, Au $p_z$.

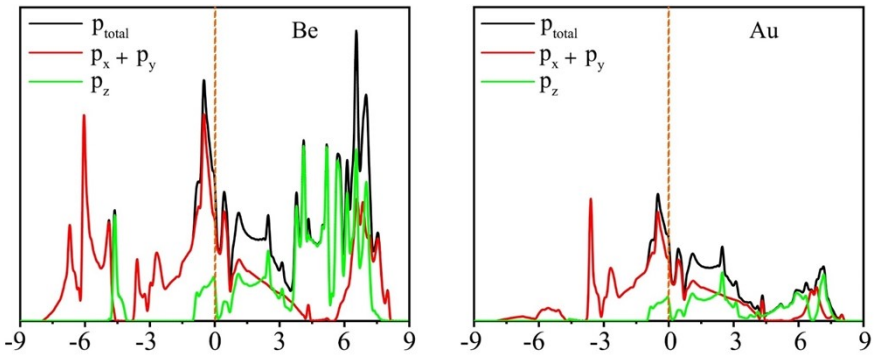


**Figure S12.** Atom-projected density of states (PDOS) of the $Be_2Au$ monolayer computed by HSE06 functional. The Fermi level is at 0 eV.

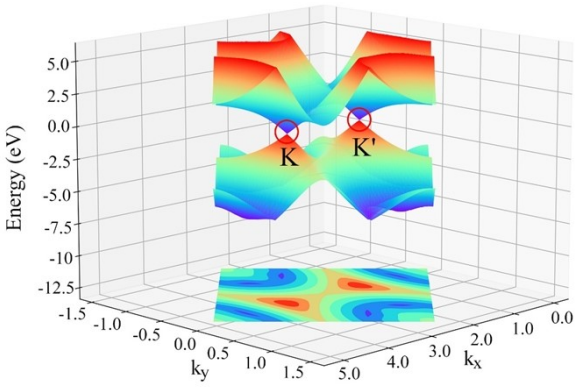


**Figure S13.** The three-dimensional band structure of the graphene.

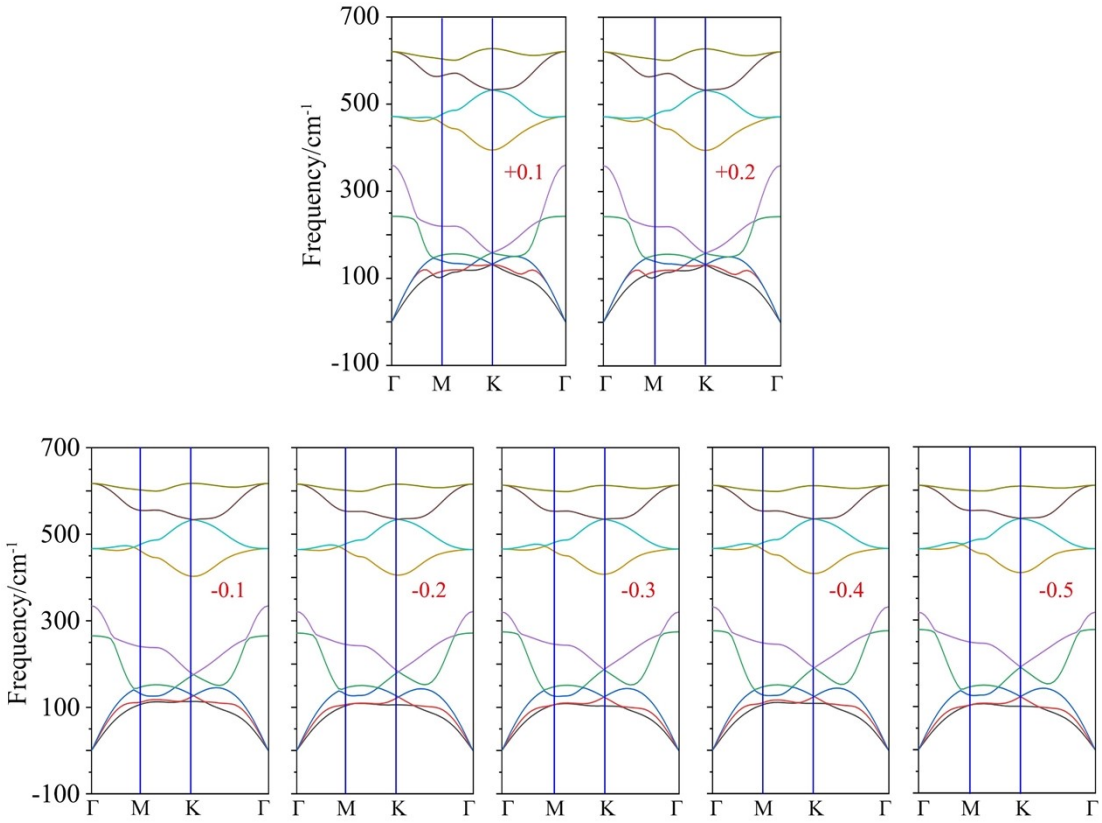


**Figure S14.** Phonon dispersion spectra for $Be_2Au$ monolayer under carrier doping from +0.2 to -0.5 electron per unit cell.

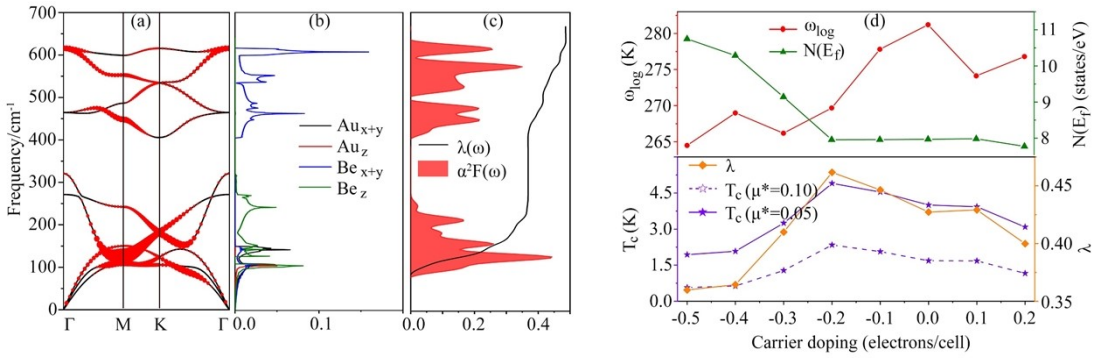


**Figure S15.** (a) Phonon dispersion with electron-phonon coupling strength, (b) phonon density of states (PhDOS), (c) Eliashberg spectral function $\alpha^2F(\omega)$ and the overall electron-phonon coupling strength $\lambda(\omega)$of the $Be_2Au$ monolayer under doping of 0.2 electrons per unit cell, and (d) evolution of the logarithmic average frequency$\omega_{log}$, the density of states at the Fermi level $N(E_f)$, the superconducting transition temperature $T_c$ and the cumulative frequency-dependent EPC $\lambda(\omega)$versus the applied carrier doping.

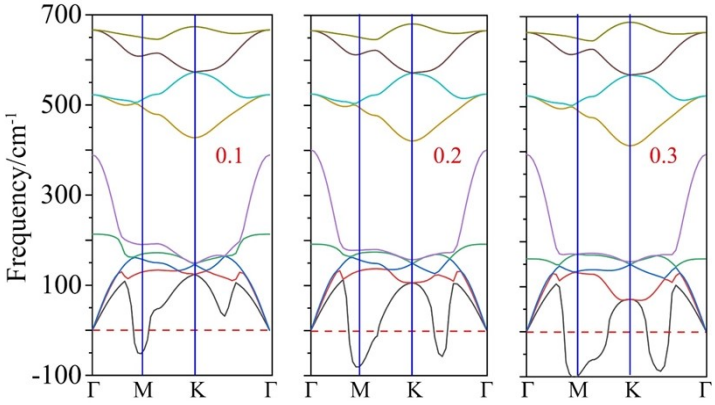


**Figure S16 (a).** Phonon dispersion spectra for $Be_2Au$ monolayer under hole doping from 0.1 to 0.3 hole per unit cell based on a strain of -1.6%.

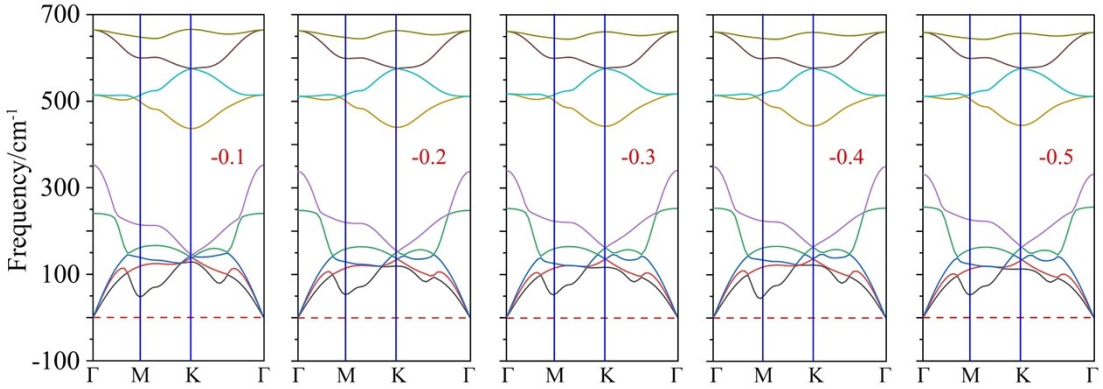


**Figure S16 (b).** Phonon dispersion spectra for $Be_2Au$ monolayer under electron doping from -0.1 to -0.5 electron per unit cell based on a strain of -1.6%.

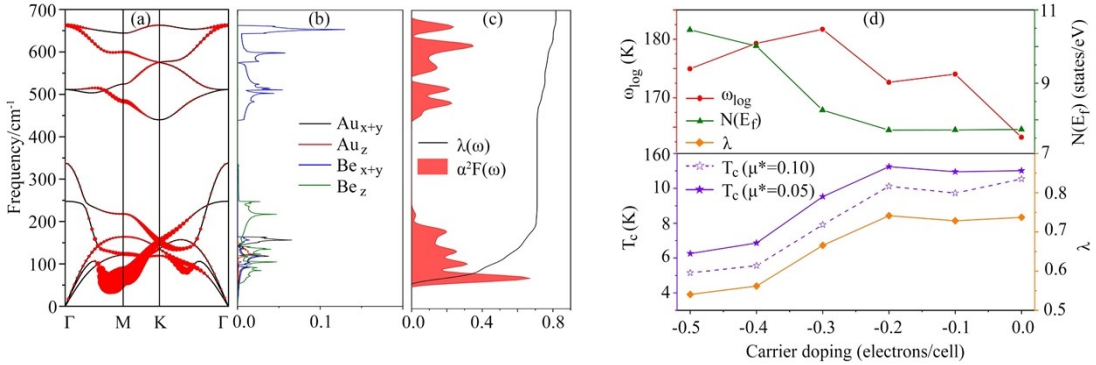


**Figure S17.** (a) Phonon dispersion with electron-phonon coupling strength, (b) phonon density of states (PhDOS), (c) Eliashberg spectral function $\alpha^2F(\omega)$ and the overall electron-phonon coupling strength $\lambda(\omega)$of the $Be_2Au$ monolayer under doping of 0.2 electrons per unit cell based on a strain of -1.6%, and (d) evolution of the logarithmic average frequency$\omega_{log}$, the density of states at the Fermi level $N(E_f)$, the superconducting transition temperature $T_c$ and the cumulative frequency-dependent EPC $\lambda(\omega)$versus the applied electron doping based on a strain of -1.6%.

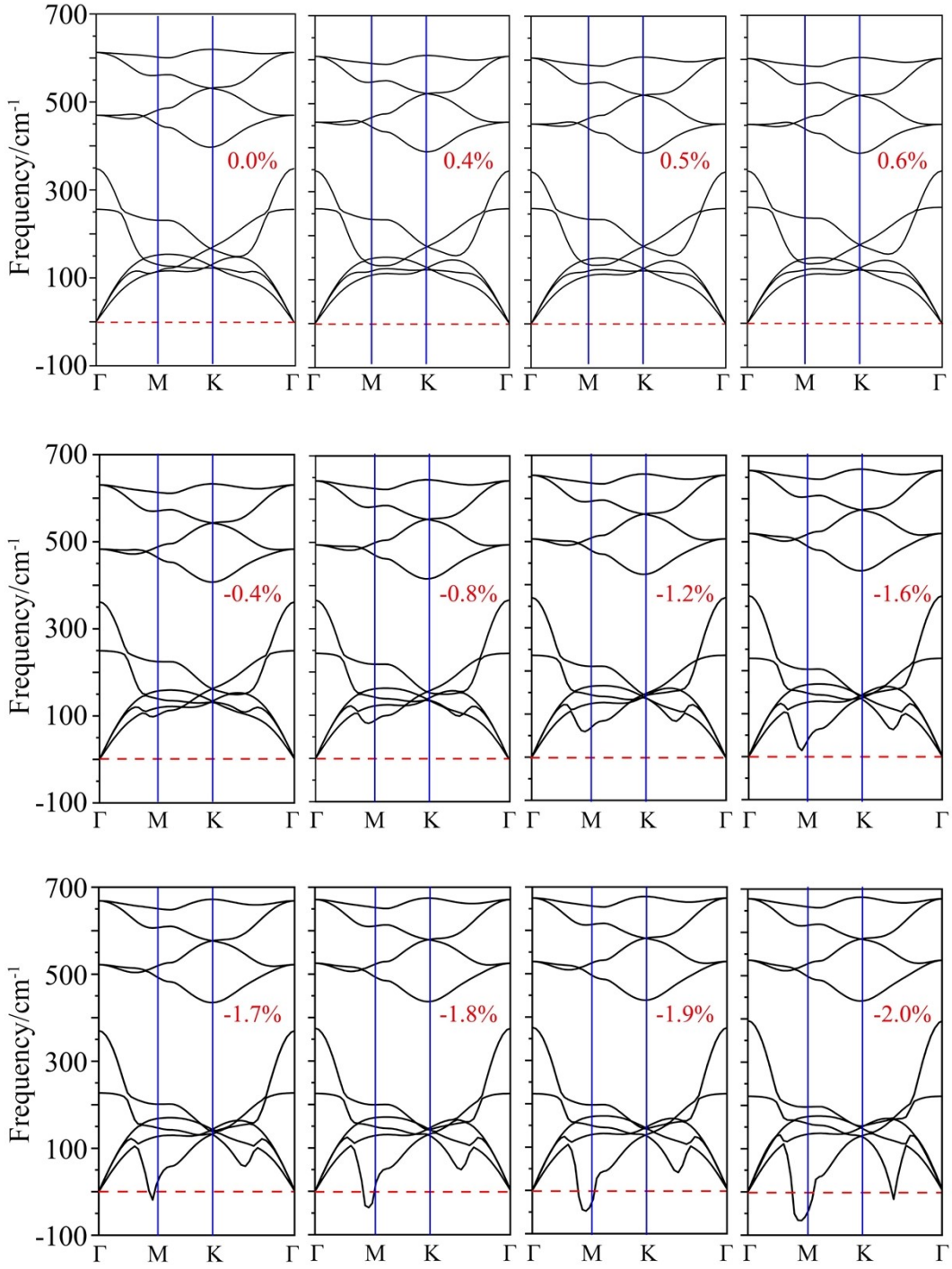


**Figure S18.** Phonon dispersion spectra for $Be_2Au$ monolayer under strain from -1.6% to 0.6%.

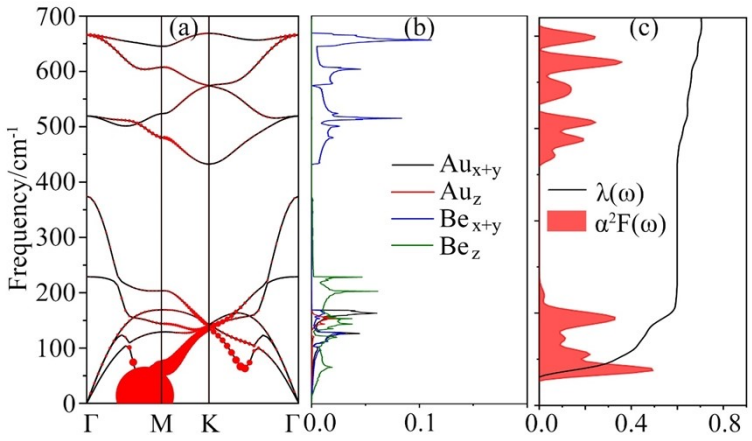


**Figure S19.** (a) Phonon dispersion with electron-phonon coupling strength, (b) phonon density of states (PhDOS), (c) Eliashberg spectral function $\alpha^2F(\omega)$ and the overall electron-phonon coupling strength $\lambda(\omega)$ of the $Be_2Au$ monolayer under strain = -1.6%.

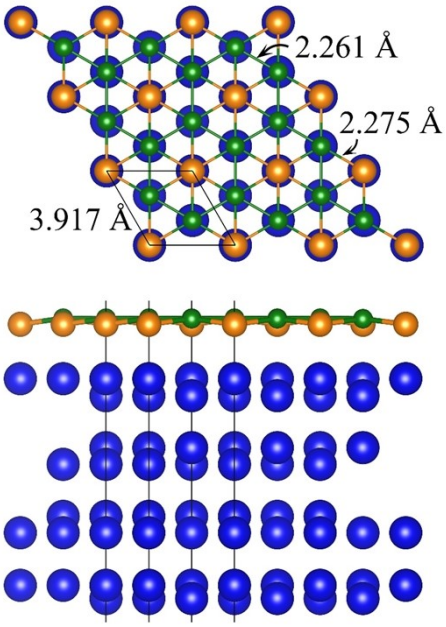


$Be_2Au$/Si(111)

**Figure S20**. Top and side views of $Be_2Au$ monolayer on Si(111) surface.